

B lifetime and $B^0\bar{B}^0$ mixing results from early Belle II data

Reem Rasheed^{*†}

University of strasbourg, CNRS, IPHC UMR 7178, F-67000 Strasbourg, France

E-mail: reem.rasheed@iphc.cnrs.fr

This paper summarizes the first results on B^0 lifetime and mixing from early phase 3 Belle II data corresponding to an integrated luminosity of $\int L = 2.7\text{fb}^{-1}$. It presents two analysis that demonstrate vertexing and tagging capabilities useful for further time-dependent CP violation measurements. The first analysis uses partially reconstructed $B^0 \rightarrow D^{*+}l\nu$ decays combined with an additional high momentum lepton in the rest of the event. The latter one uses fully reconstructed hadronic decay final states $B^0 \rightarrow D^{(*)\mp}X^\pm$.

*XXIX International Symposium on Lepton Photon Interactions at High Energies - LeptonPhoton2019
August 5-10, 2019
Toronto, Canada*

^{*}Speaker.

[†]on behalf of the Belle II collaboration

1. Introduction

The physics run of Belle II started in 25 March 2019 [1] and continued until June 30th where the integrated luminosity amount to 6.5 fb^{-1} at Y(4S) of which 0.83 fb^{-1} off-resonance. Toward the end of this period, dubbed early phase 3, SuperKEKB accelerator reached a maximum instantaneous luminosity of $1.2 \times 10^{34} \text{ cm}^{-2}\text{s}^{-1}$, while the final goal is to achieve 40 times the KEK instantaneous luminosity and integrated 50 ab^{-1} , as shown in fig 1. This paper presents performance studies and initial cross checks with data corresponding to 2.66 fb^{-1} at the Y(4S) resonance and 0.83 fb^{-1} off-resonance

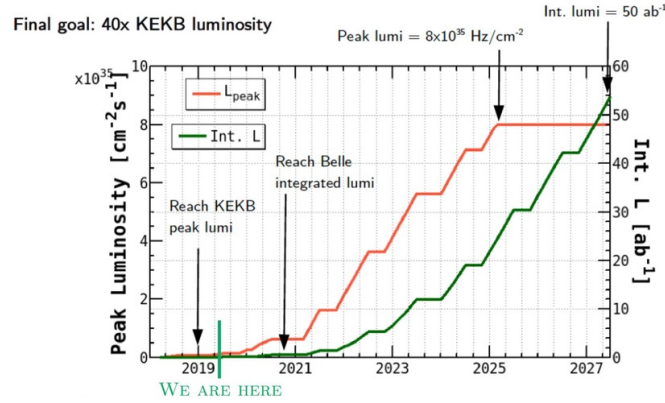


Figure 1: Expected SuperKEKB luminosity profile with time.

2. Time dependent CP violation measurements at Belle II

One of the important analysis projects of Belle II is time dependent CP violation (TDCPV) measurements, through which the CKM angles ϕ_1/β and ϕ_2/α can be accessed. Figure 2 illustrates TDCPV analysis technique in Belle II. From the electron positron collision a $B\bar{B}$ pair is produced in quantum entangled state, which constrains the two B mesons to have opposite flavors at anytime before one decays. We reconstruct the B meson decaying into a CP eigen-state noted as B_{CP} , while some of the daughters of the second B meson, denoted as B_{tag} , are used to tag both flavors at the time of the first decay. Then we measure the time difference between the decays of the two B mesons from the distance along the beam axis Δz , with $\Delta t = \frac{\Delta z}{\beta\gamma c}$. Once the time difference Δt and the flavor q (± 1 for B/\bar{B}) are determined for the set of reconstructed CP final states, the decay rate with time can be evaluated per flavor and used to extract the CP violating parameters, A_{CP} and S_{CP} , from the theoretical formula 2.1.

$$P(\Delta t, q) = \frac{e^{-\Delta t/\tau_{B^0}}}{4\tau_{B^0}} [1 + q(A_{CP} \cos(\Delta m_d \Delta t)) + S_{CP} \sin(\Delta m_d \Delta t)] \quad (2.1)$$

Thus the keys to this measurement are vertexing capability to calculate Δt and flavor tagging to obtain q , both techniques are discussed in the next sections.

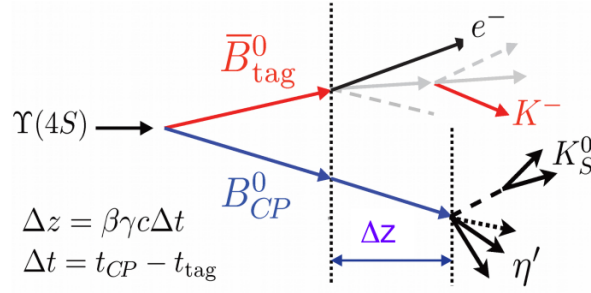


Figure 2: Illustration of the TDCPV measurement technique in Belle II (here in the $B^0 \rightarrow K_S + \eta'$ channel), benefiting from the entangled B-meson pair created in e^-e^+ collisions at SuperKEKB energy.

2.1 Vertexing in Belle II

Major improvements of Belle II detector over the Belle setup include additional two innermost pixel layers [2] and the extension of the four double-sided strip layers [3] covering up to a radius of 135 mm from the collision point. These improve the resolution on track impact parameters, in view of the reduced boost $\beta\gamma = 0.28$ compared to Belle, as well as the a more efficient K_S reconstruction at larger radii. These improvements provide better performance for analyzing TDCPV-relevant channels.

2.2 Flavor tagger

The flavor tagger [4] applies inclusive techniques based on multivariate methods to maximally exploit the information provided by the different flavor-specific signatures in flavor-specific decays. These decays were chosen for their relatively high branching fractions ($>2\%$) and lead to tagging categories shown in table 1.

Categories	Targets for \bar{B}^0	Underlying decay modes
Electron	e^-	$\bar{B}^0 \rightarrow D^{*+} \bar{\nu}_\ell \ell^-$
Intermediate Electron	e^+	$\hookrightarrow D^0 \pi^+$
Muon	μ^-	$\hookrightarrow X K^-$
Intermediate Muon	μ^+	
Kinetic Lepton	l^-	$\bar{B}^0 \rightarrow D^+ \pi^- (K^-)$
Intermediate Kinetic Lepton	l^+	$\hookrightarrow K^0 \nu_\ell \ell^+$
Kaon	K^-	
Kaon-Pion	K^-, π^+	
Slow Pion	π^+	
Maximum P*	l^-, π^-	$\bar{B}^0 \rightarrow \Lambda_c^+ X^-$
Fast-Slow-Correlated (FSC)	l^-, π^+	$\hookrightarrow \Lambda \pi^+$
Fast Hadron	π^-, K^-	$\hookrightarrow p \pi^-$
Lambda	Λ	

Table 1: Flavor tagging categories with some characteristic examples of the considered decay modes(right).

In order to extract the flavor specific signatures, discriminating variables are calculated for each particle candidate to give a specific signature that will correspond to an output of a single category called sub-tagger, on this level a multivariate method to obtain a probability output q, r , where $q = -1(+1)$ for $B^0(\bar{B}^0)$, and r the dilution factor defined as $r = 1-w$, w being the fraction of

wrong identification over the total number of tagged events, thus providing the correct flavor tag . The expected effective tagging efficiency is 37.2 % to be compared with 30 -33 % in BaBar and Belle [6]

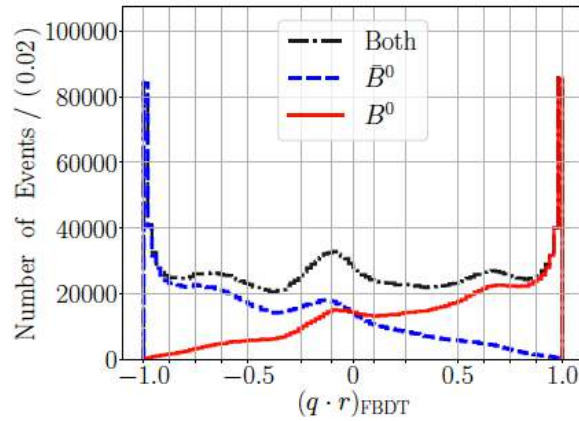


Figure 3: Flavor Tagger output extracted from [4]

3. B life time and mixing from inclusive semileptonic decays

Using a sample of partially reconstructed $B^0 \rightarrow D^{*-} l^+ \nu(l = e, \mu)$, with $D^{*-} \rightarrow \bar{D}^0 \pi^-$, we measure the $B^0\bar{B}^0$ mixing frequency in early phase 3 dataset. The analysis technique is sketched on figure 4. B meson signal candidates, B_{sig} , are selected by partial reconstruction combining only a slow pion π_s and a charged lepton l_{sig} and its flavor is determined by another single, but high momentum, charged lepton l_{tag} expected from the B_{tag} decay. It may happen that the lepton selected for tagging originates from a secondary decay as depicted on figure 4, either from the B_{tag} : l'_{tag} , either from the B_{sig} itself: l''_{tag} .

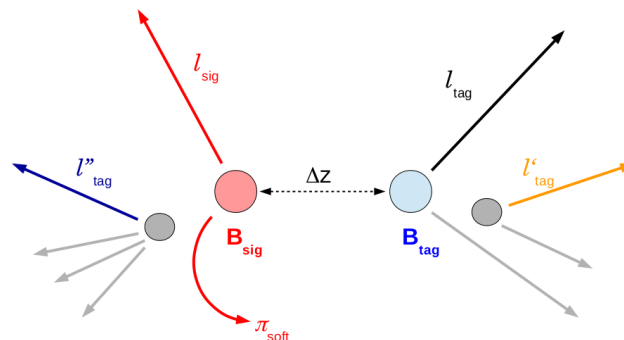


Figure 4: Measurement of B lifetime and mixing from semileptonic decays.

3.1 Time integrated analysis

In this section we report the results of the time-integrated analysis, the main goal is to evaluate the signal yields and fraction of mixed/unmixed events.

Beginning with the untagged samples (that is we only reconstruct the signal side B_{sig} candidate without requiring the presence of additional lepton candidate in the event) the number of signal events is measured from the the neutrino invariant mass M_{ν}^2 distribution. The neutrino invariant mass is computed assuming that the B_{sig} is at rest in the center-of-mass frame and using the slow pion momentum to infer the D^* momentum. Under these conditions, the distribution of correctly reconstructed events should be compatible with zero.

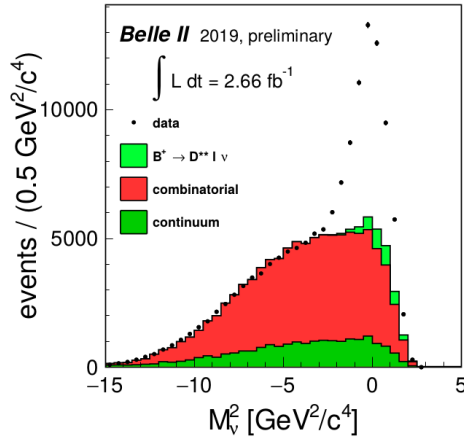


Figure 5: M_{ν}^2 distribution for untagged events in early phase 3 dataset.

Then we move to the tagged samples where a high momentum lepton l_{tag} is required, which allows to separate the selected events into two categories: mixed events with l_{sig} and l_{tag} carrying the same charge and unmixed events with opposite charge leptons. M_{ν}^2 distributions for both categories are shown on figure 6, from which we calculate the number of mixed and unmixed events, corrected for their respective inefficiencies, to extract the fraction of mixed events as:

$$\chi_d = 17.3 \pm 3.6\%, \quad (3.1)$$

to be compared with world average of 18.6 % [5].

3.2 Time dependent asymmetry

We define the time dependent asymmetry A from equation 3.2:

$$A(|\Delta t|) = \frac{N_U(|\Delta t|)}{N_U(|\Delta t|) + N_M(|\Delta t|)}, \quad (3.2)$$

where N_U is the unmixed yield and N_M the mixed yield. The distribution of A with Δt is shown in fig 7.

The left distribution presents the asymmetry in the signal region defined as $M_{\nu}^2 > -3 \text{ GeV}^2/c^4$ which shows an evidence of mixing, due to the non-flat behavior. The right one, for off-resonance data, displays a flat behavior within statistical uncertainties.

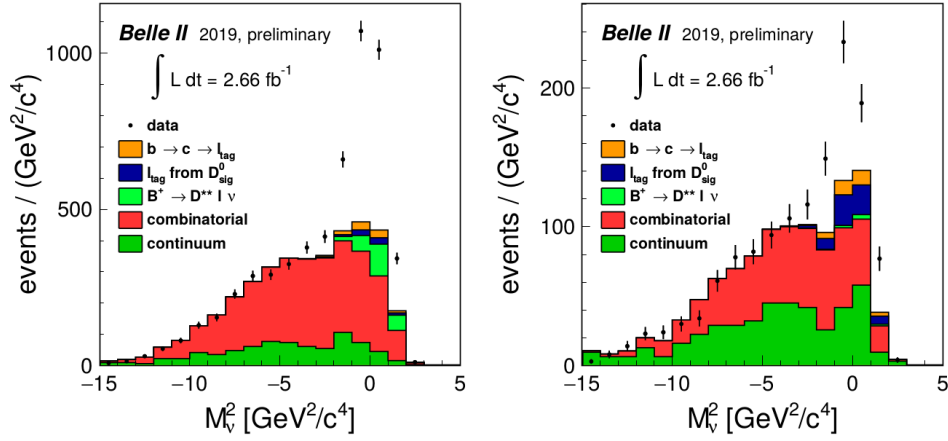


Figure 6: M_V^2 distribution for mixed events (right), and unmixed events (left).

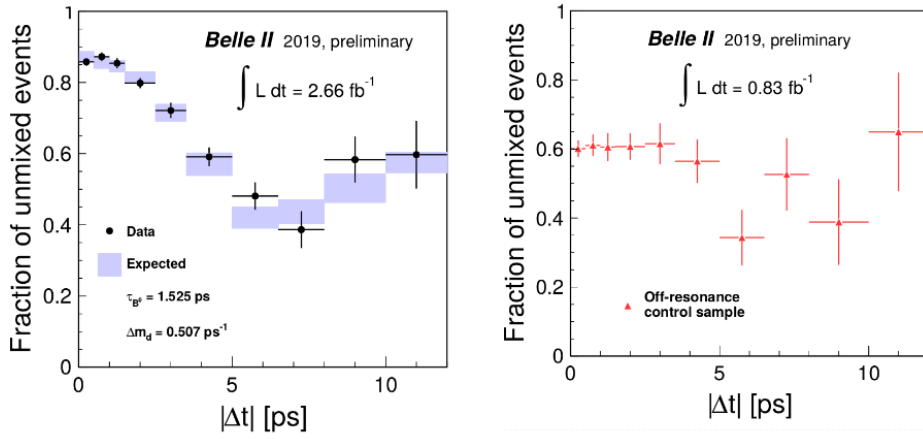


Figure 7: Time dependent asymmetry $A(|\Delta t|)$ for the $M_V^2 > -3 \text{ GeV}^2/c^4$ signal region (left) and for off-resonance data (right).

4. Preliminary results from B^0 to hadronic decays analysis

Other analysis to demonstrate Belle II vertexing capabilities are ongoing using B^0 decays to hadronic final states. These decays are self tagged channels and allows studying the performance of the flavor tagger. Figure 8 shows the beam energy substituted B meson mass m_{bc} , for each of these channels:

$$m_{bc} = \sqrt{E_{beam} - p_B^2} \quad (4.1)$$

where p_B is the center of mass frame momentum of the B meson. Only a fraction of the available luminosity have been used here for the rediscovery of these channels in the early phase 3 dataset. The full time-dependent and flavor tagged analysis is ongoing.

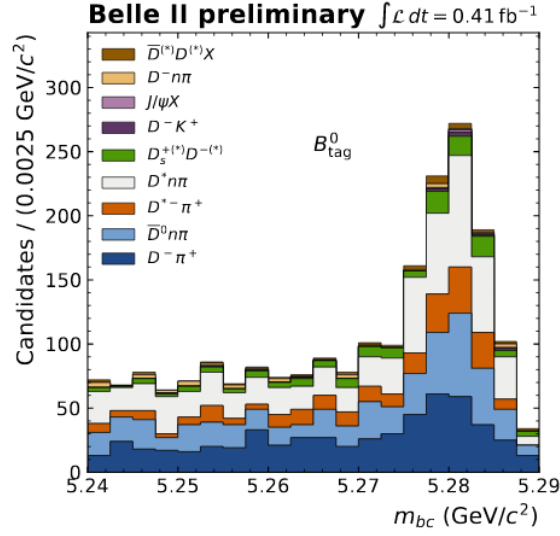


Figure 8: Beam energy substituted mass m_{bc} distribution for various self-tagged hadronic decays in phase 3 data, channels are shown on the top left of the figure.

5. Conclusions and outlooks

Belle II physics run has started, commissioning of the vertexing and flavor tagging tools are ongoing, for which performances are expected to improve with respect to Belle. Currently, our analysis of partially reconstructed semileptonic B^0 decays allowed evaluating a mixed event fraction χ_d in agreement with the world average. A second analysis started to exploit self-tagged fully reconstructed hadronic B^0 decays. Rediscovery of these channels is ongoing and will lead to detailed time-dependent and flavour-tagged studies. The final Belle II dataset of 50 ab^{-1} will provide a better room for TDCPV studies looking forward to the next decade of exciting Belle II results.

References

- [1] T. Browder, "Recent News from Belle II", to appear in PoS (LeptonPhoton) 2019,
- [2] Hans-Gunther Moser for the DEPFET collaboration, "The Belle II DEPFET pixel detector Nuclear Instruments and Methods" A,831, 85-87, (2016),
- [3] K. Adamczyk et al., "The silicon vertex detector of the Belle II experiment, Nuclear Instruments and Methods" A,824, 406-410 (2016),
- [4] The Belle II physics book, arXiv:1808.10567,
- [5] M. Tanabashi et al. (Particle Data Group), Phys. Rev. D 98, 030001 (2018),
- [6] B. Aubert et al. "The BABAR Detector: Upgrades, Operation and Performance". Nucl. Instrum. Meth. A729.1305.3560.(2012)